RESEARCH ARTICLE

INTERNATIONAL RESEARCH JOURNAL OF MULTIDISCIPLINARY TECHNOVATION

Asian Research Association

DOI: 10.54392/irjmt2637

Computational Analysis of Phloroglucinol as an Anti-Inflammatory Agent Targeting TNF-α in Rheumatoid Arthritis

Manoj Kumar Karuppan Perumal [a], K. Ragavendhar [b], R. Thirugnanasambandam [b], Mukesh Kumar Dharmalingam Jothinathan [c], Govindaraju Kasivelu [d], Remya Rajan Renuka [e, *]

[a] Centre for Stem cell Mediated Advanced Research Therapeutics, Saveetha Dental College and Hospitals, Saveetha Institute of Medical and Technical Sciences, Saveetha University, Chennai, 600 077, Tamil Nadu, India.

[b] National Facility for Coastal and Marine Research - Centre for Ocean Research, Sathyabama Institute of Science and Technology, Chennai – 600119, Tamil Nadu, India.

[c] Department of Biochemistry, Saveetha Medical College and Hospital, Saveetha Institute of Medical and Technical Sciences (SIMATS), Saveetha University, Chennai, Tamil Nadu, India.

[d] Centre for Ocean Research, Sathyabama Institute of Science and Technology, Chennai, 600 119, India

[e] Centre for Integrative Medical Research, Sree Balaji Medical College and Hospital, Bharath Institute of Higher Education and Research, Chromepet, Chennai, 600044, India.

* Corresponding Author Email: remya.praveen5@gmail.com

DOI: https://doi.org/10.54392/irjmt2637

Received: 11-11-2025; Revised: 02-03-2026; Accepted: 17-04-2026; Published: 06-05-2026

Abstract: This study utilised computational analysis to investigate the therapeutic potential of phloroglucinol against rheumatoid arthritis (RA). The Differentially expressed genes were identified from the GEO dataset GSE1919 and RA-associated targets were retrieved from the Comparative Toxicogenomics Database (CTD). By comparing these datasets, we identified 17 overlapping targets using a Venn diagram. Then, the top five genes are identified using Cytoscape and CytoHubba plugin. Gene Ontology and KEGG pathway enrichment analyses revealed involvement of these targets in inflammatory signalling. The ADME analysis through the QikProp module demonstrated favourable pharmacokinetic properties, including a molecular weight of 126.112 Da, QPlogPo/w of -0.020, oral bioavailability of 70.508% and no violation of Lipinski's Rule of Five. The molecular docking analysis indicated moderate binding affinities with key inflammatory proteins such as IL6 (-3.583) IL-10 (-2.735), IL-1β (-3.764), ICAM1 (-2.890), and TNF-α. (-4.568). The phloroglucinol-TNF-α complex was subjected to 500 ns molecular dynamics simulation, which confirmed structural stability as evidenced by RMSD values and preserved secondary structure throughout the simulation. These findings identify phloroglucinol as a promising natural small-molecule with TNF-α as its primary molecular target.

Keywords: Rheumatoid Arthritis, Phloroglucinol, Network Pharmacology, Molecular Docking, Molecular Dynamics Simulation, TNF-A, Anti-Inflammatory.

1. Introduction

Rheumatoid arthritis (RA) is a chronic autoimmune disease and driven by the activation of pro-inflammatory cytokines, which cause synovial inflammation and joint destruction [1-3]. The progression of the disease is driven by activation of inflammatory cytokines, which coordinate downstream signalling within the synovium. The activation of macrophages and synoviocytes leads to the release of TNF-α, IL-1β, and IL-6, which amplify downstream signalling through NF-κB and JAK/STAT pathways. As a result, they promote metalloproteinase expression, osteoclast activation, angiogenesis, and immune cell infiltration, ultimately leading to cartilage degradation [4].

The current therapies such as disease-modifying antirheumatic drugs (DMARDs) target these cytokines and have proven improved outcomes. These therapies are suboptimal due to limitations such as high cost, parenteral administration, infection risk, immunogenicity, and incomplete response, which remain a major challenge. These challenges support the search for novel small molecules that are capable of modulating the inflammatory pathway. The natural products and phytochemicals have also become significant in the identification of anti-inflammatory multi-target compounds with improved safety profiles [5, 6].

Phloroglucinol (1,3,5-trihydroxybenzene), a low molecular weight polyphenolic compound found in marine algae and medicinal plants, possesses

antioxidant and anti-inflammatory properties [7, 8]. Its unique properties, such as aromatic structure and multiple hydroxyl groups, make it an excellent scaffold for modulating inflammatory signals. Previous studies have demonstrated its biocompatibility in wound healing models where phloroglucinol-based hydrogels and found significant anti-bacterial activity and lower cytotoxicity against human keratinocytes [9]. Similarly, phloroglucinol extracted from Rosenvingea intricate is incorporated with PEGylated zinc oxide nanoparticles was tested against A549 lung cancer cells for enhanced therapeutic efficacy. The results exhibited that it induced apoptosis and cell cycle arrest against lung cancer cells indicating bioactivity and delivery efficiency [10]. These findings demonstrate that phloroglucinol exhibits potential therapeutic efficacy when structurally optimized or formulated. Phenolic compounds have been reported that it modulate NF-κB signalling and cytokine expression, which may upregulate the inflammatory regulators [11, 12]. However, the direct molecular interaction with RA-associated inflammatory networks remains unexplored.

RA is not activated by a single cytokine, but rather by an interconnected signalling network involving immune cell activation and downstream pathways [13]. Usually, the single-target inhibitors fail due to this and compounds that are capable of including multiple targets have significant application. Therefore, identifying hub genes and validating structural interactions with inflammatory proteins are critical in determining whether phloroglucinol exerts profound effects within RA-relevant signalling pathways [14].

In our study, we used a combined system of computation (Bioinformatics analysis of the RA-related gene expression data and network pharmacology to identify the phloroglucinol targets), molecular docking analysis to determine the binding affinity of the phloroglucinol-target complex to key inflammatory proteins, ADME to predict the drug-like characteristics of phloroglucinol, and molecular dynamics (MD) simulations to confirm the binding stability of the most promising phloroglucinol-target complex. This integrative strategy is to determine sustainable molecular targets of phloroglucinol to RA pathogenesis.

2.Materials and Methods

2.1 Data Set Retrieval

The gene expression dataset GSE1919, was retrieved from the Gene Expression Omnibus (GEO) database (https://www.ncbi.nlm.nih.gov/geo/). This public repository contains high-throughput gene expression data generated using microarray and next-generation sequencing platforms. This study selected GSE1919 because it contains gene expression for RA patients and healthy controls, analysed using the Affymetrix Human Genome U95A Array (GPL91 platform). The data consisted of synovial tissue samples from RA patients (n = 5) and healthy controls (n = 5) [15, 16]. This study included pretreatment samples and post treatment or therapy resistant samples were not included.

2.2 Pre-processing and Normalization of Microarray Data

The normalization was performed using Robust Multi-array Average (RMA) method implemented in R software (version 2.6.0) to ensure data comparability and technical variation. The RMA methods include background correction, quantile normalization, and log2 transformation of probe intensities. Through this procedure, the expression values across samples are standardized and batch-related biases.

2.3 Identification of Differentially Expressed Genes (DEGs)

DEGs analysis between RA and the healthy samples was performed using GEO2R, which applied limma (Linear Models for Microarray Data) statistical framework. To perform statistical analysis, the Benjamini and Yekutieli correction was used to regulate the false discovery rate (FDR). The genes that obtained an adjusted p-value (Padj) below 0.05 and an absolute log2 fold change ($|\log2FC|$)≥1 were viewed as significantly differentially expressed. The distribution of upregulated and downregulated genes was visualized using a volcano plot, where statistical significance ($-\log10$ p-value) was plotted against fold change (log2FC). The list of significant DEGs was downloaded from GEO2R for subsequent analyses.

2.4 RA-Associated Target Identification

The Comparative Toxicogenomics Database (CTD) was also acquired to analyse RA-associated gene targets. The DEGs obtained from GSE1919 were intersected with RA-associated genes from CTD using FunRich software (version 3.1.3). A Venn diagram was generated to visualize overlapping genes, which were considered RA-relevant candidate targets for network construction and enrichment analyses.

2.5 Protein-Protein Interaction Network Analysis

The overlapping genes were integrated into the STITCH database (http://stitch-db.org/) to examine the predicted protein-protein interactions [16, 17]. Then the interaction networks were exported and visualized in Cytoscape software (v3.5.1). Analysis of network topology was conducted with CytoHubba plugin when hub genes were rated by five centrality measures including degree, betweenness, radiality, bottleneck and

maximum clique centrality (MCC). The highest-ranking genes of these algorithms were taken to the analysis.

2.6 Functional Annotation Analysis

The functional enrichment analysis was performed using the Enrichr web tool to explore the biological relevance of the identified RA-associated target genes (https://maayanlab.cloud/Enrichr/). The diverse collection of gene set libraries is integrated in Enrichr, which applies statistical algorithms to identify significant biological terms. The gene ontology (GO) enrichment analysis is conducted on three categories, Biological Process, Cellular Component and Molecular Function [17]. The enrichment significance was calculated using the Fisher exact test, and p-values were adjusted for multiple testing using the Benjamini–Hochberg method to control the false discovery rate (FDR). GO terms with an adjusted p-value < 0.05 were considered statistically significant. Kyoto Encyclopedia of Genes and Genomes (KEGG) pathway enrichment analysis was subsequently performed using the same gene set. Pathways with an adjusted p-value < 0.05 and containing at least three enriched genes were considered significantly enriched. The top enriched GO terms and KEGG pathways were visualized using bubble charts and bar plots to represent enrichment significance and gene count distribution.

2.7 In Silico Pharmacological Analysis

2.7.1 ADME Properties Prediction

Pharmacokinetic and drug-likeness profiles of phloroglucinol were identified by Glide-XP screening and assessed with the help of Schrödinger's QikProp module. This in silico program estimates pharmaceutically relevant physicochemical properties and ADME (Absorption, Distribution, Metabolism, and Excretion) parameters for organic molecules. The study involves 35 most important descriptors such as central nervous system activity, blood-brain barrier permeation, Madin-Darby Canine Kidney (MDCK) cell permeability, and oral bioavailability in human beings [18].

2.7.2 Molecular Docking Analysis

The interactions of phloroglucinol and the major inflammatory proteins in RA studied through molecular docking to determine the binding interactions [19]. The crystal structure of IL-10 (PDB ID: 1Y6K), IL-6 (PDB ID: 7PHS), IL-1β (PDB ID: 1ITB), ICAM1 (PDB ID: 1IAM), and TNF-α (PDB ID: 5MU8) were obtained at the Protein Data Bank (https://www.rcsb.org/). Structures were prepared in Protein Prep Wizard, Maestro v14.1 (Schrodinger Suite 2024-3) using the resolutions of 2.52 Å, 2.77 Å, 1.63 Å, 1.65 Å, and 3.00 Å, which determined the structures. The co-crystallized ligands and heteroatoms were eliminated, the hydrogen atoms absent were inserted, and crystallographic water molecules further than 5.0 Å of the active site were erased. The refinement of the structures was performed at pH 7.0 by using the PROPKA program, and the energy was minimized with an RMSD cutoff of 0.30 Å by the OPLS4 force field. The phloroglucinol (CID: 359) was retrieved in SDF format in PubChem database and was prepared with the LigPrep module v7.1 of the Schrodinger Suite. The OPLS4 force field was used to optimize and minimise energy of the ligand. Epik was used to form ionization and tautomeric states at PH 7.0 +2.0 with maximum favourable conformer to dock.

The siteMap module of Schrodinger was used to predict active binding sites of the selected receptors. The dimensions of the receptor grid were 32 Å × 32 Å × 32 Å (1Y6K), 25 Å × 25 Å × 25 Å (7PHS), 29 Å × 29 Å × 29 Å (1ITB), 32 Å × 32 Å × 32 Å (1IAM), and 21 Å × 21 Å × 21 Å (5MU8). The Glide module v10.4 was used in Extra Precision (XP) mode to perform molecular docking, to determine the ideal binding pose of phloroglucinol in the receptor active sites. Hydrogen bonds, hydrophobic and electrostatic interactions were analyzed, as well as identified amino acid residues that were important in binding the ligands in the docked complexes.

2.7.3 Molecular Dynamics Simulation

Stability of the docked receptor-ligand complexes was evaluated by the use of MD simulations, which were done using the Desmond module v7.9 in the Schrodinger Suite 2024-3 [20]. The solvation of the simulation system was made with the SPC water model on the orthorhombic box of 10 × 10 × 10 Å. The OPLS4 force field was used to minimize the potential energy by neutralizing and minimizing the system. The simulations were conducted in terms of NPT ensemble at 300 K and 1.01325 bars of pressure. All simulations were 500 ns long, and trajectories were recorded at 100ps intervals, forming a 1000-frame trajectory. Dynamics and stability of each interaction between the protein and the ligand were examined using Desmond Simulation Interaction Diagram and centred on Root Mean Square Deviation (RMSD) and Root Mean Square Fluctuation (RMSF) of both protein and ligand at each time level based on the analysis.

3.Results and Discussion

3.1 Identification of Potent Targets Associated with Phloroglucinol from GSE Datasets

This study utilized the RA dataset GSE1919 obtained from GEO database. A volcano plot (Figure 1a) was illustrated to express the DEGs, which highlight the key transcriptional changes associated with RA. The volcano plot showed both statistical significance and fold-change, helping distinguish gene expression changes from noise. Only strongly expressed genes

were taken forward for further analysis [21]. The activation of inflammatory signalling pathways between normal and RA was further validated by a heat map of genes, as shown in Figure 1b. The RA- associated genes were retrieved from CTD, while DEGs were obtained from GEO datasets. These two gene sets were compared and visualized using a Venn diagram (Figure. 1c), revealing 17 overlapping targets such as GADD45A, CDKN1A, MMP3, NFKB, MCP-1, ICAM1, VCAM1, IL6, COX2, ERK1, JNK, AP1, IL10, IL1B, IL8, TNFAIP3, and TNF. Notably, the overlapping genes provide key mediators of inflammatory signalling, including pro-inflammatory cytokines, matrix-degrading enzymes and transcriptional regulators. Collectively, this multifaceted molecular dysregulation characterizes RA and provides a well-justified target for evaluating the therapeutic potential of phloroglucinol [22]. However, it is important to acknowledge that the present study was limited to only two databases, namely GEO and CTD, for target identification.

3.2 Pharmacological Networking of Phloroglucinol

The protein-protein interaction analysis was performed using STITCH database to validate the 17 potential targets (Figure 2a). The network analysis revealed an interconnected architecture, suggesting that phloroglucinol does not act through a single molecular target but rather modulates a coordinated network of functionally related proteins [23]. These targets are imported into Cytoscape to illustrate the interaction network. The CytoHubba plugin was applied to determine the key regulatory nodes within the network. Multiple topological parameters, including degree, betweenness centrality, radiality, maximal clique centrality (MCC), and bottleneck score, were evaluated to select the top 5 genes (Table 1). The integration of multiple centrality measures ensured unbiased identification of hub genes based on topological parameter may overlook nodes that functionally have modest connectivity scores [24]. The network visualization (Circular form) and topological analysis identified the most significant hub genes within the interaction network (Figure 2b and 2c). The top 5 targets, including ICAM1, IL-6, IL-10, IL-1β, and TNF-α is shown in Figure 2d.

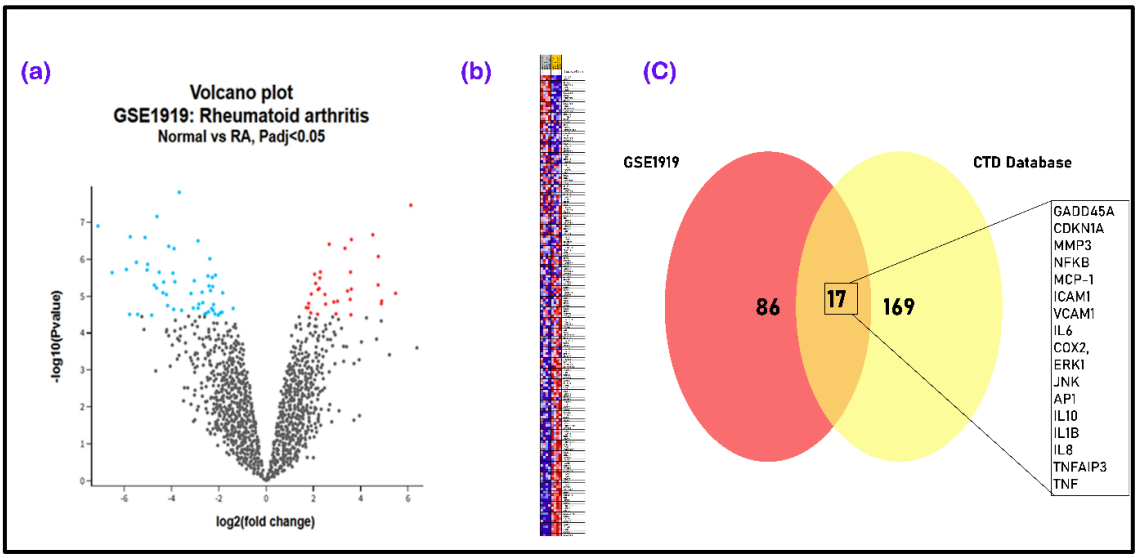

Figure 1. (a) Volcano plot showing DEGs in the GSE1919 dataset comparing normal samples and RA samples (adjusted $p < 0.05$). **(b)** Heat map illustrating the expression profile of genes from the hallmark inflammatory response gene set across normal and RA samples. **(c)** Venn diagram showing the overlap between DEGs from GSE1919 and RA-associated genes retrieved from the CTD.

Table 1. Network topology analysis of core hub genes

Top Genes	Radiality	Stress	Degree	Bottleneck
TNF	2.775	2820	27	28
IL6	2.575	840	19	7
IL10	2.375	374	16	8
IL1B	2.500	596	16	8
ICAM1	2.450	716	14	6

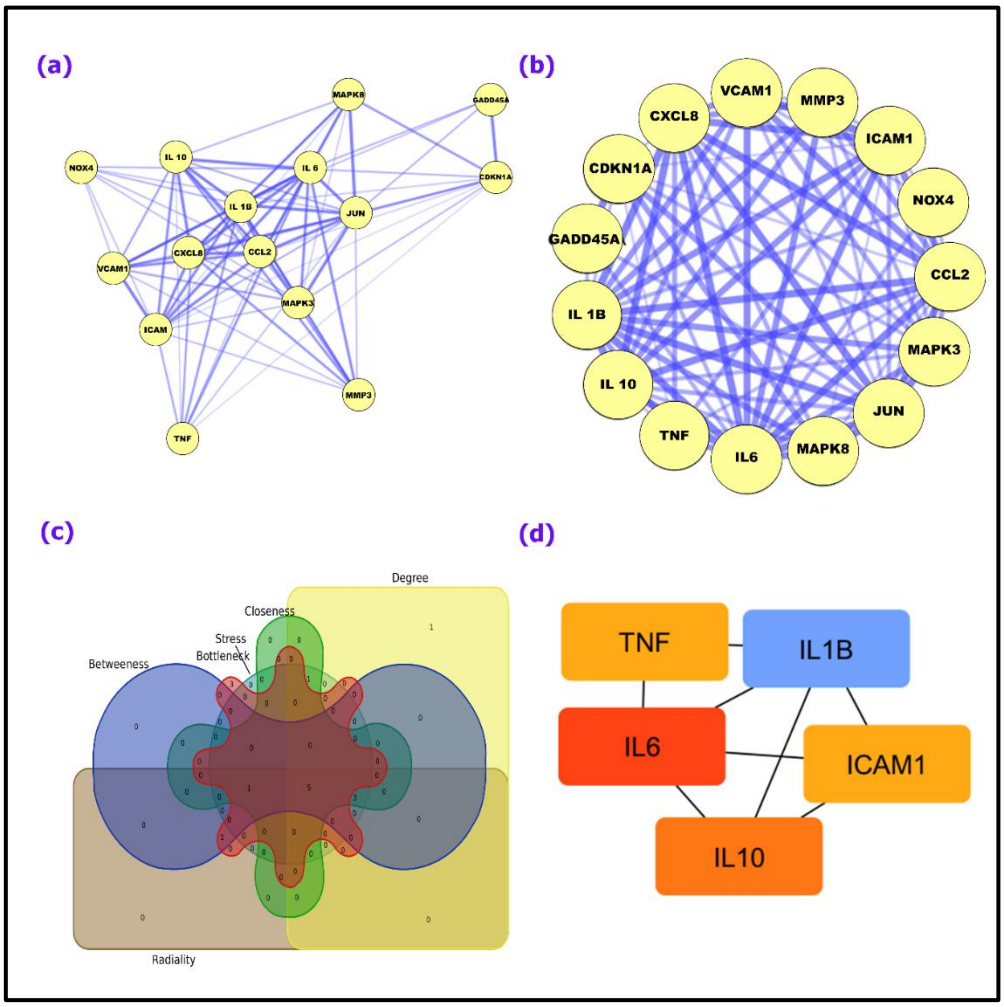

Figure 2. (a) Protein–protein interaction (PPI) network constructed using the STRING database. **(b)** Network visualization generated using Cytoscape software. **(c)** Hub gene identification using multiple topological parameters analyzed in CytoHubba. **(d)** Visualization of hub genes based on degree ranking in the PPI network.

3.3 Phloroglucinol-Related Functional Annotations

The Figure 3a presents the results of GO as bubble chart, highlighting the top five enriched terms across three GO categories: biological process (BP), cellular component (CC), and molecular function (MF). In the CC category, the enriched genes were primarily associated with subcellular structures such as podosomes, microvilli, and early endosomes, suggesting their involvement in cytoskeletal organization, membrane dynamics, and intracellular signalling. Podosomes are highly dynamic actin-rich structures implicated in cell adhesion, migration, and matrix degradation, and their dysregulation has been closely linked to inflammatory cell invasion and tissue remodelling in conditions such as RA [25]. The association with microvilli and early endosomes further suggests that the identified targets play important roles in membrane signalling and receptor internalization [26].

In the MF category, significant enrichment was observed in protein kinase regulator activity, ubiquitin protein-ligase activity, and kinase binding, indicating regulatory roles in signal transduction and post-translational modification pathways.

Further pathway-level interpretation was obtained through KEGG enrichment analysis (Figure 3b). The identified targets were significantly enriched in pathways related to RA, TNF signalling, and other inflammatory signalling cascades. Notably, several genes were also enriched in cancer-associated pathways, reflecting shared molecular mechanisms between chronic inflammation and tumorigenesis. This overlap is biologically coherent, as chronic inflammation is now widely recognized as a critical hallmark of cancer, with sustained inflammatory signalling [27]. The pathway enrichment analysis was performed using Gene Set Enrichment Analysis (GSEA) to validate further (Figure 3c). The plots showed significant enrichment of hallmark inflammatory response and TNF-α signalling via NF-κB pathways in RA samples compared with normal controls. Additionally, cytokine–cytokine receptor interaction and PI3K–AKT–mTOR signalling pathways were enriched. This indicates coordinated activation of pro-inflammatory and survival signalling cascades [28].

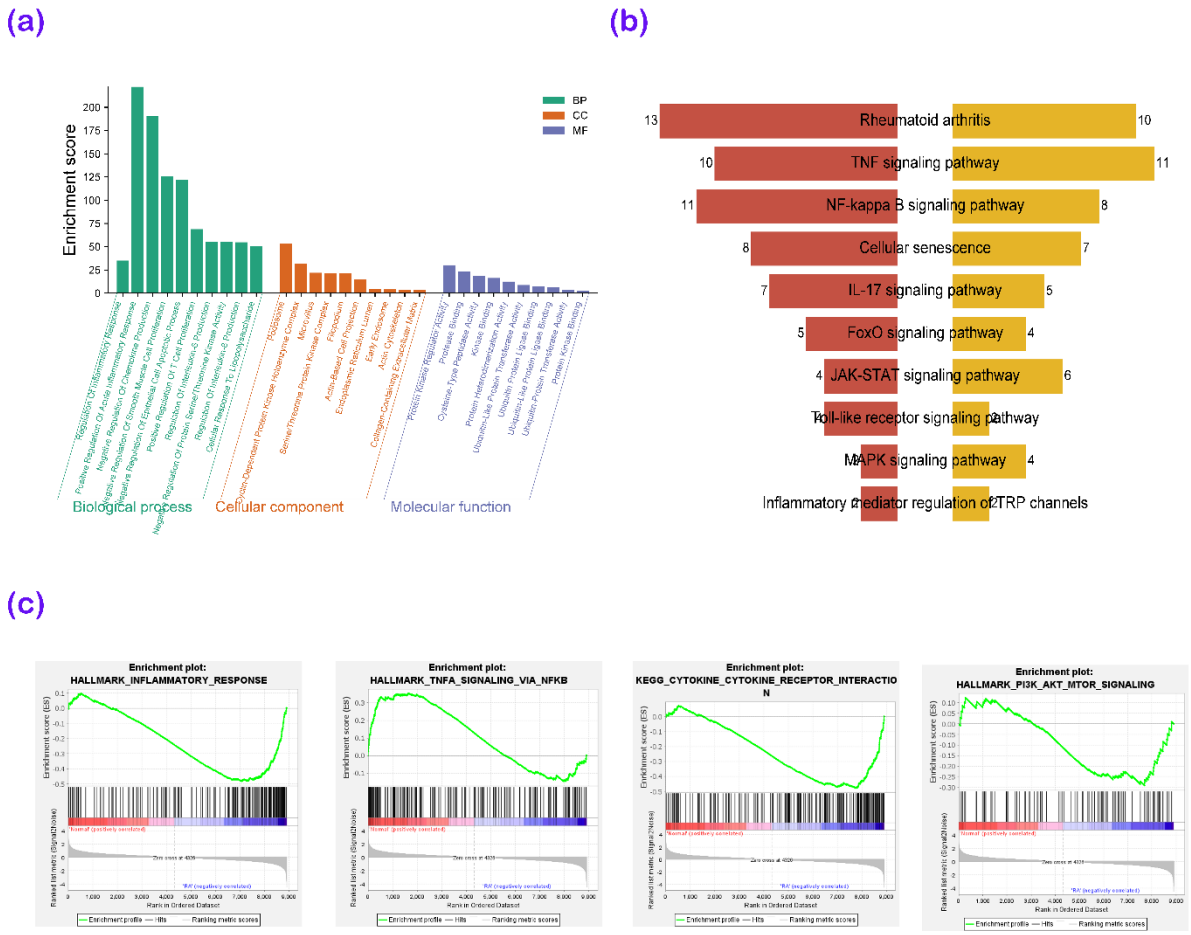

Figure 3. (a) GO enrichment analysis depicting the distribution of differentially expressed genes across biological process, cellular component, and molecular function categories. **(b)** KEGG pathway enrichment analysis illustrating the top-enriched signalling pathways associated with the identified differentially expressed genes. **(c)** GSEA plots showing the enrichment profiles of hallmark inflammatory response, TNF-α signaling via NF-κB, cytokine–cytokine receptor interaction, and PI3K–AKT–mTOR signaling pathways in RA samples compared with normal controls

3.4 ADME Properties of Phloroglucinol

The ADME analysis via QikProp module of Schrodinger accessed the potential of phloroglucinol as a therapeutic drug. The results showed that the molecular weight of the compound was 126.112 Da. Compounds with lower molecular weights generally exhibit faster absorption, better tissue penetration, and reduced efflux-mediated resistance, which are pharmacologically advantageous characteristics [29].

Phloroglucinol showed moderate lipophilicity with a QPlogPo/w of -0.020. Excessively lipophilic compounds tend to accumulate in fatty tissues and exhibit poor aqueous solubility, whereas overly hydrophilic compounds struggle to permeate biological membrane [30]. The aqueous solubility (QPlogS) was -0.362, indicating good solubility at physiological conditions. In terms of absorption properties, the QPPCaco cell permeability was 275.662 nm/sec, which shows good intestinal absorption. The oral bioavailability of phloroglucinol was estimated to be 70.508. This indicates that phloroglucinol has a moderate oral bioavailability. Its ability to passively diffuse into the membrane is further supported by the MDCK cell permeability (QPPMDCK) of 122.875 nm/sec.

The distribution showed QPlogBB of -0.868, which implied that there was limited but significant blood-brain barrier penetration. The central nervous system (CNS) activity score was found to be -1, indicating low activity in the central nervous system. This suggests that phloroglucinol is unlikely to exert significant central nervous system effects [31]. The skin permeability coefficient (QPlogKp) was -3.768 cm/hour, showing the characteristic of hydrophilic compounds. The drug-likeness analysis demonstrated no violation to the Rule of Five and rule of Lipinski. This further supported the excellent drug-like properties of the phloroglucinol. Additionally, it has three hydrogen bond donors and 2.250 hydrogen bonds acceptors, which are within limits that allow an ideal bioavailability orally. It is important to note that the compound has zero rotatable bonds (#rotor = 0), which means that the structure is rigid and might add specificity to binding, as shown in Table 2.

Table 2. Pharmacokinetics properties of Phloroglucinol

Property	Parameter	Value
Molecular Properties	Molecular Weight (mol MW)	126.112
	Dipole Moment (dipole)	0.000
	Polarizability (QPpolrz)	11.122
	Globularity (glob)	0.935
Lipophilicity	QPlogPo/w	-0.020
Solubility	QPlogS	-0.362
Absorption	QPPCaco (nm/sec)	275.662
	PercentHumanOralAbsorption (%)	70.508
Distribution	QPlogBB	-0.868
	QPPMDCK (nm/sec)	122.875
CNS Activity	CNS	-1
Metabolism	#metab	0
Membrane Permeability	QPlogKp (cm/hour)	-3.768
Surface Areas	SASA (Å²)	302.232
	FISA (Å²)	164.033
	FOSA (Å²)	0.000
	PISA (Å²)	138.200
	PSA (Å²)	67.701
	WPSA (Å²)	0.000
Drug-likeness	Rule of Five	0
	Rule of Three	0
Hydrogen Bonding	Hydrogen Bond Donors (donorHB)	3.000
	Hydrogen Bond Acceptors (accptHB)	2.250
Rotatable Bonds	#rotor	0

3.5 Molecular Docking

Phloroglucinol had a moderate binding specificity on the five inflammatory proteins targets such as IL-10, IL-6, IL-1β , ICAM, with docking scores of between -2.735 to -4.568 kcal/mol (Figure 4 and Table 3).

Among the evaluated targets, TNF-α exhibited strongest interaction with phloroglucinol having the docking scores of −4.568 kcal/mol and an MM-GBSA binding energy of −24.06 kcal/mol. This complex was stabilized by 3 hydrogen bonds, including ASP140, PRO20 and ALA22. Additionally, other hydrophobic & polar residues such as LEU142, PHE144, PRO139, GLN21, ASN19, GLN25, GLU23 were also contributed. The presence of multiple hydrogen bonds and supporting non-covalent interactions suggests moderate stabilization within the TNF-α binding region [32].

Likewise, the phloroglucinol and IL-1β complex has docking scores of -3.764 kcal/mol and an MM-GBSA binding energy of −17.4 kcal/mol. There were 2 hydrogen bonds, such as PRO56, GLY55; other interacting bonds such as ARG57, SER59, ALA60, TYR111, PRO53, PHE4 (hydrophobic & polar contacts) were also observed, indicating the minimal stabilization of the complex.

The IL-6 and phloroglucinol complex have docking scores of −3.583 kcal/mol and n MM-GBSA score of −17.66 kcal/mol. MET117 and GLY8 were the 2 hydrogen bonds formed, which might have interfered with IL-6 receptor by polar and hydrophobic interactions such as VAL118, THR116, PRO9, PRO158, GLU157 and LYS210. In the case of ICAM, the docking score was -2.890 kcal/mol with an MM-GBSA binding energy of −14.14 kcal/mol. The complex was accompanied by 4 hydrogen bonds including ASP312, ARG270, HIS222 and ARG337.The stabilising effect that may influence

the molecular activity was established by the interaction residues such as TYR184, HIS187, ALA225, PHE333, LEU217, and HIE261.

Lastly, the weakest interaction was observed in IL-10 complex with binding affinity of -2.735 and binding energy scores of −10.23 kcal/mol. The complex formed 1 hydrogen bond, namely TYR72. It has other hydrophobic interactions such as LEU94, PHE30, VAL33, VAL91, MET77 and PHE37. Likewise, the reference inhibitors (Table 4), Celecoxib and Baricitinib, showed stronger binding overall than phloroglucinol. Docking scores ranged from −2.432 to −7.554 kcal/mol, with MM-GBSA energies between −27.82 and −52.91 kcal/mol, indicating stable complex formation. The strongest interaction was observed with IL-10, particularly for Baricitinib.

Previous computational studies have reported that genes such as TNF-α, IL-6, and IL-1β are the key inflammatory mediators and primary therapeutic targets in RA [33]. Numerous docking analysis of natural molecules against these cytokines have demonstrated moderate binding affinities in the range of -3 to -6 kcal/mol [34, 35]. The docking analysis and MM-GBSA values represent computationally predicted binding affinities [36]. Similarly, in our study, the highest binding affinity among the key inflammatory targets was observed in TNF-α. This is due to the combined effect of multiple hydrogen bonds and polar interactions, which may enhance binding stabilization when compared to other targets [37]. Although this binding affinity is low in comparison to high-affinity biologics, it is similar to several small-molecule anti-inflammatory agents that are effective in the clinic [38, 39].

The phloroglucinol exhibited moderate interaction with all key inflammatory targets of RA and these scores do not confirm the biological activity. In vitro and in vivo analyses of phloroglucinol are required to confirm its functional efficacy [40]. Contrastingly, the celecoxib and baricitinib are clinically approved drugs for inflammatory proteins, and these drugs demonstrate selective binding toward the primary targets of our key inflammatory proteins used in our docking study [41].

Table 3. Molecular docking results and interaction analysis

S.No	Compound	Protein	Docking Score (kcal/mol)	MM-GBSA (kcal/mol)	Hydrogen Bond Residues	Non-Hydrogen Bond Interactions
1	Phloroglucinol	TNF-α	-4.568	-24.06	ASP140, PRO20, ALA22	LEU142, PHE144, PRO139, GLN21, ASN19, GLN25, GLU23 (hydrophobic & polar contacts)
2		IL-10	-2.735	-10.23	TYR72	LEU94, PHE30, VAL33, VAL91, MET77, PHE37 (hydrophobic interactions)
3		IL-6	-3.583	-17.66	MET117, GLY8	VAL118, THR116, PRO9, PRO158, GLU157, LYS210 (hydrophobic & polar contacts)
4		IL-1β	-3.764	-17.4	PRO56, GLY55	ARG57, SER59, ALA60, TYR111, PRO53, PHE4 (hydrophobic & polar contacts)
5		ICAM-1	-2.890	-14.14	ASP312, ARG270, ARG337, HIS222	TYR184, HIS187, ALA225, PHE333, LEU217, HIE261 (hydrophobic, polar & π interactions)

Table 4. Comparative docking scores and binding energies of standard anti-inflammatory drugs against RA-associated target proteins.

Proteins	Compound	Docking Score (kcal/mol)	Binding Energy (kcal/mol)
IL-10	Celecoxib	-7.554	-48.70
	Baricitinib	-6.548	-52.91
IL-6	Baricitinib	-3.241	-28.70
	Celecoxib	-2.432	-35.21
IL-1β	Baricitinib	-3.647	-35.09
	Celecoxib	-3.118	-30.79
ICAM-1	Baricitinib	-3.511	-28.53
	Celecoxib	-2.515	-38.64
TNF-α	Celecoxib	-3.079	-27.82
	Baricitinib	-2.808	-35.03

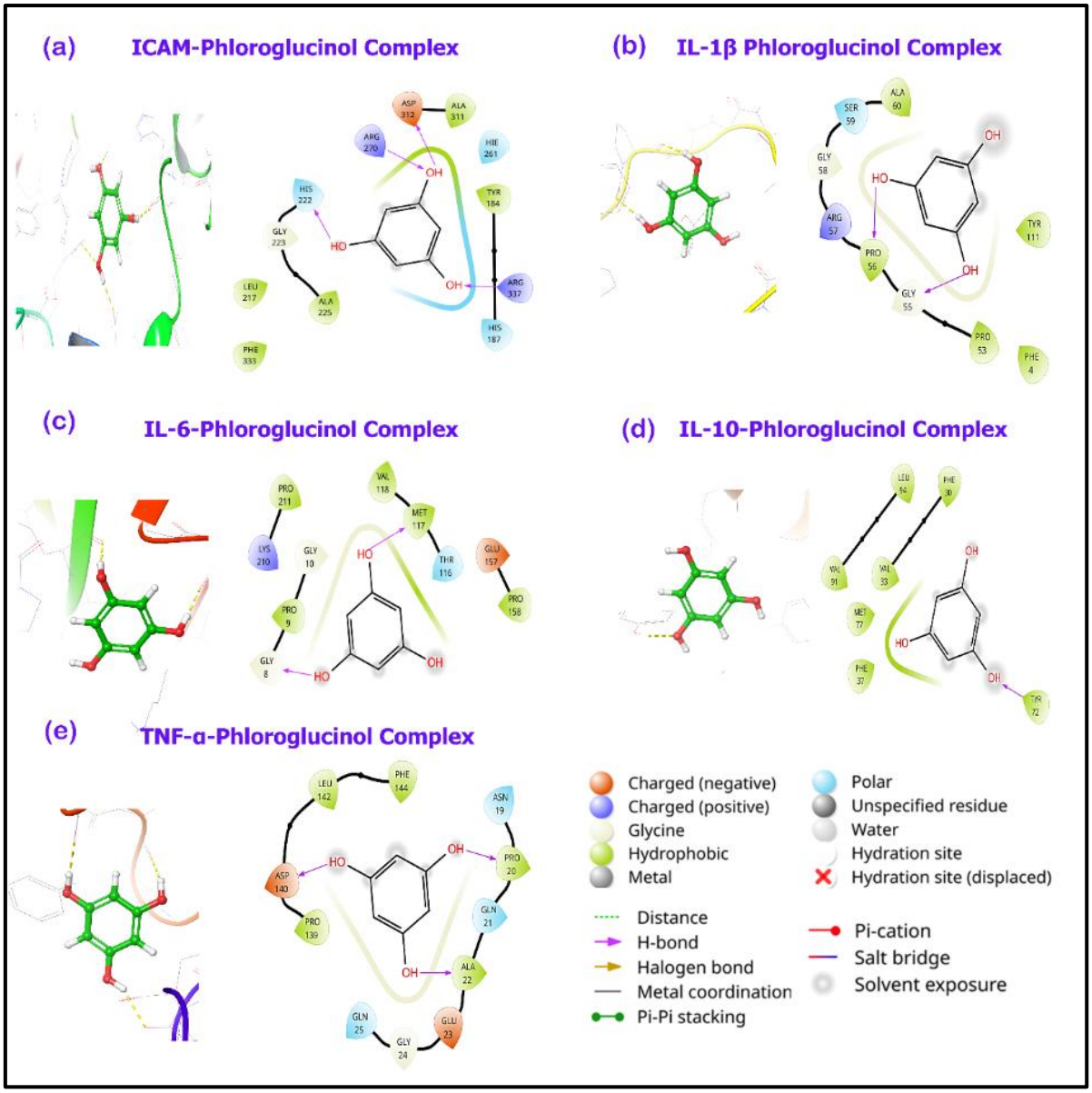

Figure 4. Molecular docking interaction diagrams of phloroglucinol with target proteins ICAM, IL-1β, IL-6, IL-10, and TNF-α.

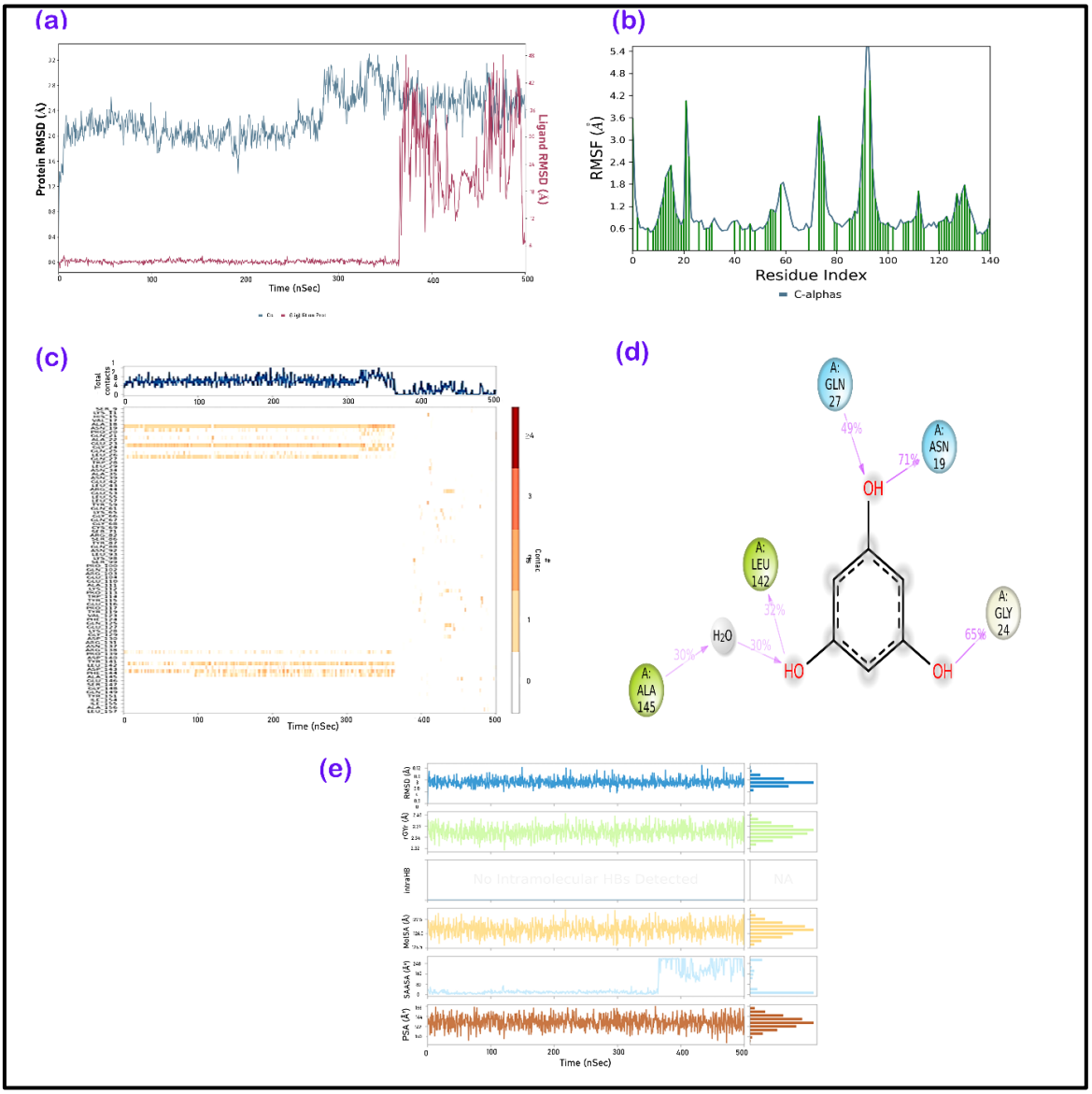

Figure 5. Molecular dynamics simulation analysis of the TNF-α–phloroglucinol complex over 500 ns. **(a)** Root Mean Square Deviation (RMSD) plot showing backbone Cα RMSD of TNF-α (blue) and ligand RMSD relative to the protein (red) as a function of simulation time (ns). **(b)** Root Mean Square Fluctuation (RMSF) profile of TNF-α Cα atoms, representing per-residue flexibility throughout the simulation. **(c)** Protein–ligand interaction timeline illustrating the persistence and type of intermolecular contacts formed during the simulation period. The top panel shows total contacts, and the lower panel displays residue-wise interaction occupancy across time. **(d)** Two-dimensional interaction diagram of phloroglucinol with key TNF-α residues, indicating hydrogen bonds and water-mediated interactions with interaction occupancy percentages. **(e)** Ligand property analysis over simulation time, including ligand RMSD, radius of gyration (rGyr), molecular surface area (MolSA), solvent-accessible surface area (SASA), and polar surface area (PSA).

3.6 MD Stimulations

The RMSD analysis for the phloroglucinol-TNFα complex was performed for 500 ns MD simulation to assess the structural stability of the protein-ligand complex (Figure 5a). The protein backbone (Cα atoms) remained stable for a transient period of the simulation and fluctuated minimally between the range of 1.8 Å to 2.8 Å. A moderate fluctuation was noted at 280-370 ns.

However, protein structure regained equilibrium and showed no evidence of unfolding. Similar RMSD ranges (2–3 Å) have been reported in MD studies of TNF-α–small molecule complexes, where such deviations indicate preserved structural integrity rather than instability [42].

Contrastingly, the ligand RMSD exhibited biphasic behaviour [43]. During its initial docking pose (0-363 ns), the phloroglucinol remained within the docking pocket and maintained the RMSD values around 3 Å. After 363 ns, the ligand RMSD was increased to 12-48 Å, suggesting the displacement from the binding site and dissociation into the solvent.

Therefore, the ligand exhibited stability for a short period and did not maintain occupancy at the binding site throughout the simulation. This behaviour is also reported in certain studies involving natural small molecules against TNFα [44].

The RMSF analysis of TNF α, shown in Figure 5b. The results exhibit low fluctuation values within 0.5-1.2 Å, indicating the structural stability initially. The highest fluctuations are observed at regions around 18-22, 75-80 and 92-100, with the largest fluctuation 5Å occurs at the 92-100 region. These regions correspond to solvent-exposed loop segments commonly reported as flexible in TNF-α structures [45, 46].

The protein–ligand contact timeline (Figure 5c) provides residue-level insight into the temporal stability of the phloroglucinol–TNF-α complex during the 500 ns simulation. The total contact profile analysis highlights that the ligand maintained an average of 6-10 contacts with TNF-α, indicating a stable binding phase from 0-370 ns. Beyond 370 ns, the total contacts decreased to zero with only short-lived interaction observed at the end of the simulations. The residue-wise analysis of the contact heatmap reveals the simple patterns and confirms that the interactions were primarily contained in two regions of the protein. ASN19, GLY24, GLN24, GLN27, and LEU26 were the first region residues that displayed occupancy till 370 ns. These residues are the primary anchoring region of the ligand. The second region residues include ASP140, LEU142, PHE144, and ALA145 that stabilize from the opposite side of the binding pocket. Importantly, at residue regions 18-27, there was a complete loss of binding. At 370 ns, the interaction bands disappeared and only intermittent contacts were detected. This indicates the dissociation was associated with the loss of key anchoring interactions.

Similarly, 2D interactions (Figure 5d) showed that hydrogen bonding is the dominant stabilizing interaction during the simulation. The weak role of the ionic interactions indicates that polar and water-mediated contacts are the major binding forces [47]. The LEU142 and ALA145 are the hydrogen bonds with interacting fractions of 32 and 30%, respectively. These contacts indicate the presence of bridging water molecules that contribute to stabilization of the ligand for a short time in the pocket environment [48]. The ASN 19 and GLN 27 are polar interactions, indicating that phloroglucinol hydroxyl groups are crucial for binding affinity, forming stable hydrogen bonds with TNF-α [49].

The ligand property analysis (Figure 5e) indicated that ligand RMSD remained low and stable during the initial phase (0-363 ns), fluctuating between 0.04-0.10 Å. This indicates that the phloroglucinol retained its docked confirmation within the binding pocket. But after 363 ns, there was complete displacement into the solvent, which increased in variability. Similarly, the radius of gyration (rGyr) remained constant throughout the simulation with minimal fluctuation of 2.32-2.40 Å. There was no significant expansion or compaction even after ligand dissociation. This distribution confirms that the ligand maintains its aromatic geometry and that the dissociation event is not associated with intramolecular deformation [50]. Likewise, no intramolecular hydrogen bonds (intraHB) were detected during the trajectory. This is consistent with the small size and substitution pattern of phloroglucinol, indicating that ligand stability is governed by intermolecular hydrogen bonding with protein residues and solvent molecules. The molecular surface area (MolSA) shows minor fluctuations within approximately 126–128 Å², indicating stable van der Waals surface characteristics throughout the trajectory. No abrupt shifts are observed after dissociation, supporting structural integrity of the ligand. The solvent-accessible surface area (SASA) remains relatively low and stable (20–60 Å²) during the bound phase (0–363 ns), reflecting partial burial within the binding pocket. After 363 ns, SASA increases sharply to approximately 150–250 Å², indicating substantial solvent exposure followed by ligand displacement [51]. This transition directly correlates with the loss of protein–ligand contacts and increased ligand RMSD. The polar surface area (PSA) fluctuates within a narrow range of approximately 160–168 Å², remaining stable throughout the simulation. The absence of major PSA variation further confirms that the ligand does not undergo structural rearrangement during binding or after dissociation. However, several limitations should be acknowledged. The simulation was performed using a single docking pose and a single protein conformation, which may not capture alternative binding orientations or allosteric interactions [52].

In addition, computational predictions cannot fully replicate the complex cellular microenvironment or cooperative effects present in vivo [53]. Therefore, the present findings provide structural insight into interaction feasibility but require experimental validation to confirm inhibitory potential.

4.Conclusion

In this study, the therapeutic potential of phloroglucinol against RA was studied using computational analysis. The results identified 17 potential targets associated with RA by comparing CTD database and GSE1919 dataset. The network pharmacology analysis discovered top 5 genes such as ICAM1, IL-6, IL-10, IL-1β, and TNF-α as the principal hub targets for RA. The GO and KEGG enrichment analyses confirmed involvement of these targets in RA-relevant inflammatory signalling pathways, while ADME profiling demonstrated favourable characteristics such as molecular weight of 126.112 Da, oral bioavailability of 70.508%, and no violation with Lipinski's Rule of Five. Furthermore, molecular docking analysis exhibited

moderate binding affinities ranging from -2.735 to -4.568 kcal/mol, with TNF-α exhibiting the strongest interaction, supported by an MM-GBSA binding energy of -24.06 kcal/mol. The molecular dynamics simulation for 500 ns confirmed initial binding stability up to 363 ns, after which ligand dissociation was observed, suggesting that structural optimization may be necessary to improve binding durability. The future studies should focus on in vitro and in vivo validation through cytokine inhibition assays and collagen-induced arthritis models to confirm the biological efficacy and safety profile of phloroglucinol.

References

[1] M. Jahid, K.U. Khan, R.S. Ahmed, Overview of Rheumatoid Arthritis and Scientific Understanding of the Disease. Mediterranean Journal of Rheumatology, 34(3), (2023) 284–291. https://doi.org/10.31138/mjr.20230801.oo

[2] Y. Velmurugan, S.R. Natarajan, N. Chakkarapani, S. Jayaraman, H. Madhukar, R. Venkatachalam, In Silico and in Vitro Studies for the Identification of Small Molecular Inhibitors from Euphorbia Hirta Linn for Rheumatoid Arthritis: Targeting TNF-A-Mediated Inflammation. Molecular Diversity, 29(2), (2025) 1189-1206. https://doi.org/10.1007/s11030-024-10900-1

[3] A.K. Pandarathodiyil, K.H. Shree, B. Sivapathasundharam, R. Ramadoss, Salivary Biomarker Profile in Rheumatoid Arthritis and its Interlinkage in Oral Manifestations: A Comprehensive Review. Journal of Oral and Maxillofacial Pathology, 29(1), (2025) 117-126. https://doi.org/10.4103/jomfp.jomfp_23_24

[4] L. Caliogna, M. Berni, C. Torriani, M.E. Mancuso, M.N.D. Di Minno, A.M. Brancato, E. Jannelli, M. Mosconi, G. Pasta, Pathogenesis of osteoarthritis, rheumatoid arthritis, and hemophilic arthropathy: The role of angiogenesis. Haemophilia, *30*(6), (2024) 1256-1264. https://doi.org/10.1111/hae.15097

[5] Y.H. Gonfa, F.B. Tessema, A. Bachheti, N. Rai, M.G. Tadesse, A. Nasser Singab, K.K. Chaubey, R.K. Bachheti, Anti-Inflammatory Activity of Phytochemicals from Medicinal Plants and their Nanoparticles: A review. Current Research in Biotechnology, 6, (2023) 100152. https://doi.org/10.1016/j.crbiot.2023.100152

[6] H.A. Saleh, M.H. Yousef, A. Abdelnaser, The Anti-Inflammatory Properties of Phytochemicals and Their Effects on Epigenetic Mechanisms Involved in TLR4/NF-/kB-Mediated Inflammation. Frontiers in Immunology, 12, (2021)606069. https://doi.org/10.3389/fimmu.2021.606069

[7] R.T. Polez, M.A. Ajiboye, M. Osterberg, M.M. Horn, Chitosan Hydrogels Enriched with Bioactive Phloroglucinol for Controlled Drug Diffusion and Potential Wound Healing. International Journal of Biological Macromolecules, 265, (2024) 130808. https://doi.org/10.1016/j.ijbiomac.2024.130808

[8] B. Pradhan, R. Nayak, P.P. Bhuyan, S. Patra, C. Behera, S. Sahoo, J.S. Ki, A. Quarta, A. Ragusa, M. Jena, Algal Phlorotannins as Novel Antibacterial Agents with Reference to the Antioxidant Modulation: Current Advances and Future Directions. Marine Drugs, 20(6), (2022) 403. https://doi.org/10.3390/md20060403

[9] X. Huang, J. Yang, R. Zhang, L. Ye, M. Li, W. Chen, Phloroglucinol Derivative Carbomer Hydrogel Accelerates MRSA-Infected Wounds Healing. International Journal of Molecular Sciences, 23(15), (2022) 8682. https://doi.org/10.3390/ijms23158682

[10] S. Muthu, M. Lakshmikanthan, E. Edward-Sam, M. Subramanian, L. Govindan, A.B.M. Patcha, K. Krishnan, N. Duraisamy, S. Jeyaperumal, A.T. Aziz, Encapsulation of Phloroglucinol from Rosenvingea Intricata Macroalgae with Zinc Oxide Nanoparticles against A549 Lung Cancer Cells. Pharmaceutics, *16*(10), (2024) 1300. https://doi.org/10.3390/pharmaceutics16101300

[11] M.M. Kim, S.K. Kim, Effect of Phloroglucinol on Oxidative Stress and Inflammation. Food Chemical Toxicology, 48(10), (2010) 2925–33. https://doi.org/10.1016/j.fct.2010.07.029

[12] A. Mieszkowska, L. Martocq, A. Koptyug, M.A. Surmeneva, R.A. Surmenev, J. Naderi, M. Muchova, K.A. Gurzawska-Comis, T.E. Douglas, Anti-Inflammatory and Osteogenic Effect of Phloroglucinol-Enriched Whey Protein Isolate Fibrillar Coating on Ti-6Al-4V Alloy. Polymers, 17(11), (2025) 1514. https://doi.org/10.3390/polym17111514

[13] Y. Gao, Y. Zhang, X. Liu, Rheumatoid Arthritis: Pathogenesis and Therapeutic Advances. MedComm, 5(3), (2024) e509. https://doi.org/10.1002/mco2.509

[14] H.M.U. Rana, H. Nisar, J. Prajapati, D. Goswami, R. Rawat, V. Eyupoglu, S. Shahid, A. Javaid, W. Nisar, Integrative Bioinformatic Analysis to Identify Potential Phytochemical Candidates for Glioblastoma. *Heliyon*, 10(24), (2024). https://doi.org/10.1016/j.heliyon.2024.e40744

[15] M.K. Gatasheh, S.R. Natarajan, R. Krishnamoorthy, T.S. Alsulami, P. Rajagopal, C.P. Palanisamy, V.P. Veeraraghavan, S. Jayaraman, Molecular Analysis to Identify Novel Potential Biomarkers as Drug Targets in Colorectal Cancer Therapy: An Integrated Bioinformatics Analysis. Molecular & Cellular Oncology, 11(1), (2024.) 2326699. https://doi.org/10.1080/23723556.2024.2326699

[16] Y. Chen, H. Li, L. Lai, Q. Feng, J. Shen, Identification of Common Differentially Expressed Genes and Potential Therapeutic Targets in Ulcerative Colitis and Rheumatoid Arthritis. Frontiers in Genetics, 11, (2020) 572194. https://doi.org/10.3389/fgene.2020.572194

[17] Y. Velmurugan, N. Chakkarapani, S.R. Natarajan, S. Jayaraman, H. Madhukar, R. Venkatachalam, PPI Networking, In-Vitro Expression Analysis, Virtual Screening, DFT, and Molecular Dynamics for Identifying Natural TNF-A Inhibitors for Rheumatoid Arthritis. Molecular diversity, (2025) 1-20. https://doi.org/10.1007/s11030-025-11158-x

[18] R. Roy, M.F. Sk, N.A. Jonniya, S. Poddar, P. Kar, Finding potent inhibitors against SARS-CoV-2 main protease through virtual screening, ADMET, and molecular dynamics simulation studies. Journal of Biomolecular Structure and Dynamics, 40(14), (2022) 6556-6568. https://doi.org/10.1080/07391102.2021.1897680

[19] Y. Velmurugan, S.R. Natarajan, N. Chakkarapani, S. Jayaraman, H. Madhukar, and R. Venkatachalam, In Silico and in Vitro Studies for the Identification of Small Molecular Inhibitors from Euphorbia Hirta Linn for Rheumatoid Arthritis: Targeting TNF-A-Mediated Inflammation. Molecular Diversity, 29(2), (2025) 1189-1206. https://doi.org/10.1007/s11030-024-10900-1

[20] S. Manandhar, R. Sankhe, K. Priya, G. Hari, B.H. Kumar, C.H. Mehta, U.Y. Nayak, K.S.R. Pai, Molecular Dynamics and Structure-Based Virtual Screening and Identification of Natural Compounds as Wnt Signaling Modulators: Possible Therapeutics for Alzheimer's Disease. Molecular Diversity, 26(5), (2022) 2793-2811. https://doi.org/10.1007/s11030-022-10395-8

[21] S.R. Natarajan, R. Krishnamoorthy, M.A. Alshuniaber, T.S. Alsulami, M.K. Gatasheh, P. Rajagopal, C.P. Palanisamy, R. Govindan, V.P. Veeraraghavan, S. Jayaraman, ABCE1 Facilitates Tumour Progression Via Aerobic Glycolysis and Inhibits Cell Death in Human Colorectal Cancer Cells through the P53 Signalling Pathway. Scientific Reports, 15(1), (2025) 24674. https://doi.org/10.1038/s41598-025-92436-4

[22] A. Eswaran, S.R. Natarajan, S. Jayaraman, J.M. Khan, S. Jasmine, V.P. Veeraraghavan, Jervine-Induced Suppression of Triple-Negative Breast Cancer (TNBC) Cells Growth through the Regulation of Wnt Signaling Pathway-An In-Silico and In-Vitro Approach. Journal of Computer-Aided Molecular Design, 40(1), (2026) 57. https://doi.org/10.1007/s10822-025-00754-6

[23] P. Balhara, S. Sharma, N. Vasudeva, Unraveling the chemistry, Pharmacological Activities, and Medicinal Utilization of Phloroglucinol: A Comprehensive Review. Pharmacological Research-Natural Products, (2025) 100421.https://doi.org/10.1016/j.prenap.2025.100421

[24] K. Krishnamoorthy, S.R. Natarajan, V.P. Veeraraghavan, S. Jayaraman, Blueberry Extract and its Bioactive Compounds Mitigate Oxidative Stress and Suppress Human Lung Cancer Cell (A549) Growth by Modulating the Expression of P53/EGFR/STAT3/IL6-Mediated Signaling Molecules. Cell Biochemistry and Function, 42(4), (2024) e4027. https://doi.org/10.1002/cbf.4027

[25] C. Luxenburg, S. Winograd-Katz, L. Addadi, B. Geiger, Involvement of Actin Polymerization in Podosome Dynamics. Journal of cell science, 125(7), (2012) 1666-1672. https://doi.org/10.1242/jcs.075903

[26] M.M. Postema, N.E. Grega-Larson, L.M. Meenderink, M.J. Tyska, PACSIN2-Dependent Apical Endocytosis Regulates the Morphology of Epithelial Microvilli. Molecular biology of the cell, 30(19), (2019) 2515-2526. https://doi.org/10.1091/mbc.E19-06-0352

[27] D. Fu, Z. Hu, X. Xu, X. Dai, Z. Liu, Key Signal Transduction Pathways and Crosstalk in Cancer: Biological and Therapeutic Opportunities. *Translational oncology*, 26, (2022) 101510. https://doi.org/10.1016/j.tranon.2022.101510

[28] G. Ramarajyam, R. Murugan, S. Rajendiran, Network Pharmacology and Bioinformatics Illuminates Punicalagin's Pharmacological Mechanisms Countering Drug Resistance in Hepatocellular Carcinoma, Human Gene, 42, (2024) 201328. https://doi.org/10.1016/j.humgen.2024.201328

[29] Q. Li, C. Kang, Mechanisms of Action for Small Molecules Revealed by Structural Biology in Drug Discovery. International Journal of Molecular Sciences, 21(15), (2020) 5262. https://doi.org/10.3390/ijms21155262

[30] M. Markovic, S. Ben-Shabat, A. Aponick, E.M. Zimmermann, A. Dahan, Lipids and Lipid-Processing Pathways in Drug Delivery and Therapeutics. International Journal of Molecular Sciences, 21(9), (2020) 3248. https://doi.org/10.3390/ijms21093248

[31] J. Kim, J. Won Choi, H. Jeong Kim, B. Kim, Y. Kim, E. Hwejin Lee, R. Kim, J. Kim, J. Park, Y. Jeong, J.H. Park, Phloroglucinol Derivatives Exert Anti-Inflammatory Effects and Attenuate Cognitive Impairment in LPS-Induced Mouse Model. ChemMedChem, 19(17), (2024) e202400056. https://doi.org/10.1002/cmdc.202400056

[32] P.M. Swamy, P.H. Somashekar, S.A. Shivamurthy, S. Shadakshari, M. Puttaswamappa, N.S. Shanthappa, Design, Synthesis, and Insilico Evaluation of 2-Aminothiazole Derivatives as Potential Mtor and EGFR Inhibitors. Discover Molecules, 2(1), (2025) 31. https://doi.org/10.1007/s44345-025-00039-3

[33] P.P. Pal, A.S. Begum, S.A. Basha, H. Araya, Y. Fujimoto, New Natural Pro-Inflammatory Cytokines (TNF-A, IL-6 And IL-1β) and Inos Inhibitors Identified from Penicillium Polonicum through in Vitro and in Vivo Studies. International Immunopharmacology, 117, (2023) 109940. https://doi.org/10.1016/j.intimp.2023.109940

[34] N.J. Basha, K.T. Akshay, R.M. Mohan, M. Javeed, O.M. Sharma, Synthesis, Molecular Docking, Drug Likeness, In Silico Toxicity and DFT Studies of Small Molecules as P53-MDM2 Interaction and COX-2 Dual Inhibitors. Journal of Molecular Structure, 1322, (2025) 140393. https://doi.org/10.1016/j.molstruc.2024.140393

[35] S.K. Maurya, R. Mishra, Molecular Docking Studies of Natural Immunomodulators Indicate their Interactions with the CD40L of CD40/CD40L Pathway and CSF1R Kinase Domain of Microglia. Journal of Molecular Modeling, 28(4), (2022) 101. https://doi.org/10.1007/s00894-022-05084-0

[36] M. Taylor, J. Ho, MM/GBSA Prediction of Relative Binding Affinities of Carbonic Anhydrase Inhibitors: Effect of Atomic Charges and Comparison with Autodock4Zn. Journal of Computer-Aided Molecular Design, 37(4), (2023) 167-182. https://doi.org/10.1007/s10822-023-00499-0

[37] H. Zhou, J. Zhou, Y. Lu, H. Luo, W. Hu, J. Xie, X. Wu, B. Li, S. Fan, Y. Chen, F. Zhang, Naringin Alleviates Knee Osteoarthritis by Targeting TNF-α and PTGS2: An Integrated Network Pharmacology, Molecular Simulation, and Experimental Validation Study. International Journal of Molecular Sciences, 27(4), (2026) 1812. https://doi.org/10.3390/ijms27041812

[38] S. Butala, L. Castelo-Soccio, R. Seshadri, E.L. Simpson, J.J. O'Shea, T. Bieber, A.S. Paller, Biologic Versus Small Molecule Therapy for Treating Moderate to Severe Atopic Dermatitis: Clinical Considerations. The Journal of Allergy and Clinical Immunology: In Practice, 11(5), (2023) 1361-1373. https://doi.org/10.1016/j.jaip.2023.03.011

[39] S. Xue, Y. He, L. Pei, H. Xu, Progress of Biologics and Small Molecule Drugs in the Treatment of Hidradenitis Suppurativa. The Journal of Dermatology, 52(9), (2025) 1337-1350. https://doi.org/10.1111/1346-8138.17874

[40] D. Ramirez, J Caballero, Is It Reliable to Use Common Molecular Docking Methods for Comparing the Binding Affinities of Enantiomer Pairs for their Protein Target. International journal of molecular sciences, 17(4), (2016) 525. https://doi.org/10.3390/ijms17040525

[41] S. Shams, J. M. Martinez, J. R. D. Dawson, J. Flores, M. Gabriel, G. Garcia, A. Guevara, K. Murray, N. Pacifici, M. V. Vargas, T. Voelker, J. W. Hell, J. F. Ashouri, The Therapeutic Landscape of Rheumatoid Arthritis: Current State and Future Directions. Frontiers in Pharmacology, 12, (2021) 680043. https://doi.org/10.3389/fphar.2021.680043

[42] D. Boyenle, T. I. Adelusi, A. T. Ogunlana, R. A. Oluwabusola, N. O. Ibrahim, A. Tolulope, O. S. Okikiola, B. L. Adetunji, I. O. Abioye, A. K. Oyedele, Consensus Scoring-Based Virtual Screening and Molecular Dynamics Simulation of Some TNF-alpha Inhibitors. Informatics in Medicine Unlocked, 28, (2021) 100833. https://doi.org/10.1016/j.imu.2021.100833

[43] Z. Su, Y. Wu, Computational Simulations of TNF Receptor Oligomerization on Plasma Membrane. Proteins Structure Function and Bioinformatics, 88(5), (2019) 698–709. https://doi.org/10.1002/prot.25854

[44] D. S. Chan, H. Lee, F. Yang, C. Che, C. C. L. Wong, R. Abagyan, C. Leung, D. Ma, Structure-Based Discovery of Natural-Product-like TNF-α Inhibitors. Angewandte Chemie International

Edition, 49(16), (2010) 2860–2864. https://doi.org/10.1002/anie.200907360

[45] S. Liang, J. Dai, S. Hou, L. Su, D. Zhang, H. Guo, Structural Basis for Treating Tumor Necrosis Factor α (TNFα)-Associated Diseases with the Therapeutic Antibody Infliximab. Journal of Biological Chemistry, 288, (2013) 13799–13807. https://doi.org/10.1074/jbc.M112.433961

[46] S. Yang, S. Kar, Protracted Molecular Dynamics and Secondary Structure Introspection to Identify Dual-Target Inhibitors Of Nipah Virus Exerting approved Small Molecules Repurposing. Scientific Reports, 14(1), (2024) 3696. https://doi.org/10.1038/s41598-024-54281-9

[47] S. Kubik, When molecules meet in water—Recent Contributions of Supramolecular Chemistry to the Understanding of Molecular Recognition Processes in Water. ChemistryOpen, 11(4), (2022) e202200028. https://doi.org/10.1002/open.202200028

[48] D. Chen, N. Oezguen, P. Urvil, C. Ferguson, S. M. Dann, T. C. Savidge, Regulation of Protein-Ligand Binding Affinity by Hydrogen Bond Pairing. Science Advances, 2(3), (2016) e1501240. https://doi.org/10.1126/sciadv.1501240

[49] Y. Voynikov, Phloroglucinol α-pyrones from Helichrysum: A review on Structural Diversity, plant Distribution and Isolation. Plants, 14(22), (2025) 3460. https://doi.org/10.3390/plants14223460

[50] G. Jeyaraj, B. Yang, K. Sathishkumar, S. Chokkakula, B. O. Almutairi, W. Xie, Pharmacogenomic and in Silico Identification of Isoform-Selective AKT Inhibitors from Pithecellobium dulce for precision Cancer Therapy. Frontiers in Pharmacology, 16, (2026) 1744408. https://doi.org/10.3389/fphar.2025.1744408

[51] Y. Velmurugan, S. R. Natarajan, N. Chakkarapani, S. Jayaraman, H. Madhukar, R. Venkatachalam, In silico and in Vitro Studies for the Identification of Small Molecular Inhibitors from Euphorbia Hirta Linn for Rheumatoid Arthritis: Targeting TNF-α-Mediated Inflammation. Molecular Diversity, 29(2), (2024) 1189–1206. https://doi.org/10.1007/s11030-024-10900-1

[52] A. Saleem, I. Gul, A. Hassan, J. M. Muneeb, M. Khan, A. A. Malik, B. S. Kumar, S. Singh, In Silico Molecular Docking and Molecular Dynamics Simulation Studies of Potential Inhibitors of Canine Lysyl Oxidase. Heliyon, 12(1), (2025) e44425. https://doi.org/10.1016/j.heliyon.2025.e44425

[53] S. Varalakshmi, P. Vijayalakshmi, V. Rajendran, Advancement of an (in vitro/ex vivo) Hybrid Model Framework to Forecast Polyviral Lung Disease Outcomes. Journal of Investigative Medicine, (2025) 10815589251382266. https://doi.org/10.1177/10815589251382266

Authors Contribution Statement

Manoj Kumar Karuppan Perumal: Methodology, Investigation, Writing – Original Draft. K. Ragavendhar: Formal Analysis, Visualization, Software. R. Thirugnanasambandam: Formal Analysis, Validation, Software. Mukesh Kumar Dharmalingam Jothinathan: Supervision, Writing – Review & Editing. Govindaraju Kasivelu: Supervision, Writing – Review & Editing. Remya Rajan Renuka: Conceptualization, Supervision, Writing – Review & Editing. All authors have read and agreed to the published version of the manuscript.

Funding

The authors declare that no funds, grants or any other support were received during the preparation of this manuscript.

Competing Interests

The authors declare that there are no conflicts of interest regarding the publication of this manuscript.

Data Availability

The data supporting the findings of this study can be obtained from the corresponding author upon reasonable request.

Has this article screened for similarity?

Yes